Stage-I Interstitials in Electron-Irradiated Tungsten*

J. A. DiCarlo,† C. L. Snead, Jr., and A. N. Goland
Brookhaven National Laboratory, Upton, New York 11973
(Received 3 September 1968)

Single crystals and polycrystalline 5-mil tungsten wires of high purity were irradiated at 20°K with 2.5-MeV electrons. Stage-I defect behavior was studied by internal friction, dynamic Young's-modulus, and resistivity measurements. The friction and modulus samples were electrostatically driven at their fundamental flexural mode (~600 Hz). After irradiation, a prominent but transient internal-friction peak was observed at 30°K. Simultaneous resistivity and mechanical-property measurements during isochronal annealing indicates that the friction peak recovers during a major close-pair recovery substage, and that long-range interstitial motion occurs between 45 and 100°K. Arguments are presented which identify the stress-induced ordering of the interstitial members of close Frenkel pairs as the source of the 30°K relaxation peak. Single-crystal results on relaxation strength versus stress direction suggest that the interstitials are not ⟨111⟩ but most probably are ⟨110⟩ split interstitials. Defect asymmetry and activation energies for reorientation (E_r=0.066 ±0.01 eV) and annealing (E_a=0.11±0.01 eV) are determined for the 30°K process. A discussion of internal-friction background increase with heavy irradiation is also presented.

I. INTRODUCTION

THEORETICAL studies using computer techniques have predicted that the self-interstitial in a bcc lattice possesses a "split" configuration in which two atoms are symmetrically split in a ⟨110⟩ direction about a vacant normal lattice site.[1] Because the atomic distortions surrounding a point defect of this type have a lower symmetry than that of the host lattice, the defect's existence and configuration are experimentally determinable from such lattice properties as internal friction, magnetic aftereffect, and anelastic aftereffect.[2] For example, contrary to the computer results, magnetic aftereffect studies on neutron-irradiated α iron indicate that the local distortions around the Stage-I iron interstitial are largest in the ⟨100⟩ directions.[3] The purpose of the present research was to use internal friction to detect the Stage-I interstitial in tungsten and to determine its configuration. Simultaneous measurements of resistivity and dynamic modulus were also made to augment and clarify the friction results. The interstitial defects were introduced at 20°K with 2.5-MeV electrons from the Brookhaven Dynamitron.

The detection of point defects by internal friction is based on the interaction of an applied alternating stress with the "asymmetric" strain fields of the defects.[4] Because of the external stress, defect lattice positions which were energetically equivalent under zero stress conditions split in energy, resulting in a redistribution of defect population among the available positions. This stress-induced ordering of defects within the crystal gives rise to irreversible mechanical energy losses which are observable as internal friction and an associated change in modulus, viz.,

$$\delta=\pi\Delta_0\frac{\omega\tau_r}{1+(\omega\tau_r)^2}, \tag{1}$$

$$\frac{\Delta M}{M}=\Delta_0\frac{1}{1+(\omega\tau_r)^2}. \tag{2}$$

Here δ is the log decrement, M the dynamic Young's modulus, Δ_0 the relaxation strength, ω the angular frequency of the applied stress, and τ_r the relaxation time for the asymmetric defect to reorient. Thus, the internal friction will reach a maximum when $(\tau_r)^{-1}=\omega$, that is, when the rate of defect reorientation equals the angular frequency of the applied stress. In general, the reorientation process is thermally activated, i.e.,

$$\tau_r=\tau_{r0}\exp[E_r/kT], \tag{3}$$

where E_r and τ_{r0} are the reorientation activation energy and the relaxation time for zero activation energy, respectively. Therefore, as temperature is increased, τ_r will decrease. In the present study, external alternating uniaxial stresses were obtained by vibrating 5-mil cantilevered tungsten wires in flexure at their fundamental mode of about 600 Hz.

The geometrical nature of a point defect's configuration can be determined from the relaxation strength of the internal friction contributed by the defect. Nowick and Heller[5] have studied the theoretical aspects of this problem quite extensively, especially for defects in a cubic lattice. Their results can be generalized by

$$\Delta_0=\frac{Cv_0M^{[hkl]}}{9kT}\psi_{\langle uvw\rangle}{}^{[hkl]}, \tag{4}$$

where C is the total atomic fraction of defects, v_0 the atomic volume, $[hkl]$ the crystallographic direction of

* Work supported by the U. S. Atomic Energy Commission.
† Present address: NASA, Lewis Research Center, Cleveland, Ohio.
[1] R. A. Johnson, *Diffusion in Body-centered Cubic Metals* (American Society for Metals, Ohio, 1965), p. 357.
[2] See, for example, A. C. Damask and G. J. Dienes, *Point Defects in Metals* (Gordon and Breach Science Publishers, Inc., New York, 1963), pp. 180–183.
[3] P. Moser, Mem. Sc. Rev. Met. 63, 343 (1966); 63, 431 (1966).
[4] See, for example, B. S. Berry and A. S. Nowick, in *Physical Acoustics*, edited by W. P. Mason (Academic Press Inc., New York, 1966), Vol. IIIA, p. 1.
[5] A. S. Nowick and W. R. Heller, Advan. Phys. 12, 251 (1963).

the applied uniaxial stress, and ψ a parameter proportional to the maximum stress-induced energy difference between defect positions. The magnitude of ψ is dependent both on stress direction and on the degree of anisotropy of the defect's strain field. The notation $\langle uvw \rangle$ is employed to characterize the directions for the maximum atomic distortion surrounding the defect positions. Therefore, defect geometry can be experimentally determined by comparing the observed dependence of Δ_0 on stress direction with the theoretical dependence calculated for different possible defect configurations. For example, the application of theory to single-crystal Δ_0 data on the Snoek peak in α iron[6] indicates that the carbon interstitials occupy octahedral sites, producing maximum distortion in the $\langle 100 \rangle$ directions.

II. EXPERIMENTAL PROCEDURE

The three types of single-crystal tungsten wires employed in the relaxation strength experiments were supplied with a quoted purity of 99.999% by Aremco Products, Inc. During small amplitude flexural vibration, the stress distribution in a wire is essentially undirectional along the wire length, varying linearly in magnitude from maximum tension to maximum compression across the wire diameter. For this reason each single-crystal type was grown so that it had either the [100], [110], or the [111] crystallographic direction along its wire length. Thus relaxation-strength measurements on the irradiated crystals could quantitatively indicate the relative interactions between the [100], [110], and [111] uniaxial external stresses and the anisotropic strain field of the interstitial. From back-reflection Laue photographs it was determined that each wire was indeed a single crystal, and that the direction along its length was within 3° of the crystallographic direction desired for that sample.

The polycrystalline tungsten samples, supplied by Westinghouse Corp., were obtained from drawn single-crystal rod. Whereas the single-crystal samples were used only for the relaxation-strength data, the polycrystalline wires were employed for simultaneous internal-friction and resistivity measurements. Prior to mounting, the polycrystalline wires were vacuum annealed for 1 h at 1500°C in order to remove the cold-working effects of the drawing process. The procedure employed to mount all samples was found to contribute negligible cold working to the premounting treatments. After mounting, the residual resistivity ratio of the polycrystalline wires was greater than 1000, indicating a purity of 99.995% or better for these samples.[7]

The sample holder for the simultaneous internal-friction and resistivity measurements during irradiation and annealing is shown in Fig. 1. This holder was mounted on a sample block at the bottom of a liquid-helium irradiation cryostat. The internal-friction sample, about 1 cm long, was electrostatically driven at its resonant frequency f, by applying an alternating voltage at $f/2$ between it and a nearby copper drive plate. The 2-mil-thick drive plate was maneuvered by the drive-plate manipulator until in its final position it was parallel to the sample and about 5 mils behind it with respect to the incident beam. For the relaxation-strength experiments another sample holder was employed which consisted of two juxtapositioned single-crystal internal-friction samples, each with its own drive plate and manipulator. To maximize thermal conduction on the sample block, all samples were connected to their copper holder by silver paint and a bolted copper clamp. To minimize cold working and external friction contributed by the copper clamp, all internal-friction samples were cemented to the holder above the clamp with Sauereisen insolute cement.[8]

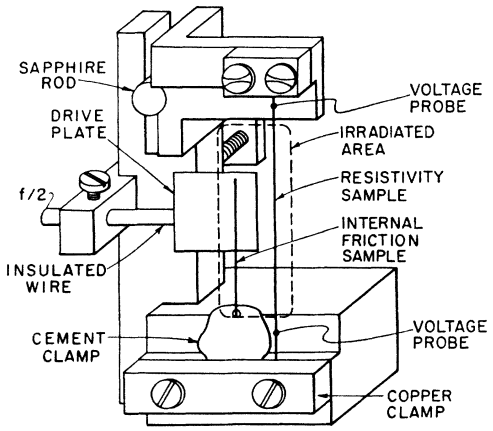

FIG. 1. Schematic of copper sample holder for simultaneous internal-friction and resistivity measurements.

As shown in Fig. 2, the detection of the mechanical vibrations of the internal-friction sample was accom-

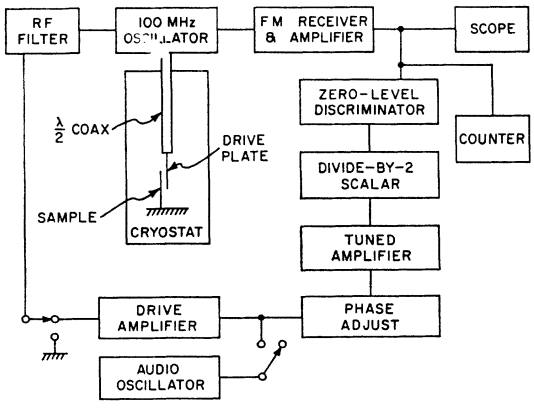

FIG. 2. Block diagram of electronic loop employed to maintain the sample vibrating at resonance.

[6] L. J. Dijkstra, Philips Res. Rept. 2, 357 (1947).
[7] H. Schultz, Acta Met. 12, 649 (1964).
[8] D. R. Muss, thesis, University of Pittsburgh, 1961 (unpublished).

plished by electrically placing the capacitor arrangement formed by the sample and drive plate into the tank circuit of a 100-MHz oscillator. Sample vibrations produced an oscillating capacitance which directly frequency modulated the rf oscillator via a half-wavelength coaxial cable. An FM tuner was used to detect these modulations and convert them back to an audio signal with a frequency f and an amplitude directly proportional to that of the sample. The internal friction, measured by the log decrement δ, was obtained by grounding the drive signal and photographing the sample's free decay on an oscilloscope screen. The error in δ was estimated to be $\pm 3\%$. All measurements were made in the high vacuum of the helium-cryostat jacket ($<10^{-6}$ mm Hg) and at vibration strains below 10^{-6} where no amplitude dependence was observed.

The dynamic Young's modulus was obtained from the resonant frequency of the sample by the relation[9]

$$f=\frac{0.14D}{l^2}\left(\frac{M}{d}\right)^{1/2}, \tag{5}$$

where D, l, and d are the sample diameter, length, and density, respectively. The block diagram of Fig. 2 indicates the closed loop which was devised to automatically maintain the sample vibrating at resonance. The sinusoidal output signal of the FM tuner was fed into a zero-level discriminator, a divide-by-two scalar, and a high-Q (~ 25) tuned amplifier, where it was converted to a square wave of frequency f, a square wave of $f/2$, and finally a sinusoidal wave of $f/2$, respectively. After passing through a phase adjust, a variable-gain audio amplifier, and an rf filter, the final signal was impressed upon the drive plate closing the loop. The initial sample motion was induced by a 1-sec pulse from a commercial audio oscillator tuned to $f/2$. The rf filter served to isolate the tank circuit from the drive circuit components, whereas the tank-circuit inductor ($\sim 0.2\ \mu$H) served to short the audio drive signal to ground before reaching the rf oscillator transistor. Resonant-period measurements were made to 8 places by counting 10^4 periods (~ 20 sec) on a Hewlett-Packard 5245 Counter. At constant temperature and for 10^4 periods the stability of the oscillating loop was determined to be ± 3 parts in 10^7 for a sample decrement of 10^{-4}. The absolute error in determining the resonance condition with the phase adjust was estimated as ± 1 part in $10^2\delta^{-1}$.

Resistivity was measured using standard potentiometric techniques. Voltage probes consisted of 1-mil constantan wires arc butt-welded onto the 5-mil resistivity samples. Due to limitations in the design of the helium irradiation cryostat, the minimum sample temperatures ranged from 11 to 15°K. For this reason all resistivity measurements were made at a base temperature of 17°K using an automatic temperature controller with better than ± 0.05°K control. With a sample current of 200 mA the resistivity error, due primarily to fluctuating thermal emf's, was less than $\pm 10^{-11}\ \Omega$ cm.

Temperature was measured with a calibrated germanium thermometer and a secondary platinum thermometer imbedded in the copper sample holder. The potential drops across the thermometers were continuously observed on a 5-place digital voltmeter. Absolute temperature accuracy was better than ± 0.1°K. During annealing treatments sample-block heating was accomplished by a 5-W control and a 300-W auxiliary heater. Cooling of the sample block by the liquid helium was accomplished via helium gas at a pressure slightly above 1 atm. For the 20 min isochronal anneal runs, manual heater control achieved the last 5°K before the anneal temperature in about 2 min. At temperature the automatic controller maintained control to better than ± 0.03°K. Upon heater shutdown the first 5°K of quench was achieved in less than 3 min.

Electron irradiations were performed in the vacuum of the accelerator. Uniform irradiations were achieved by magnetically scanning the 2.5-MeV electron beam in two directions with an average operating beam current density of 1.5 μA/cm^2. Although current was measured with a Faraday cup immediately behind the samples, the integrated dose measurements may be low by as much as 10% due to beam spreading caused by the drive plate. However, the error in the relative dose measurements was estimated to be less than 1%. Sample temperatures during irradiation were kept at 20°K by monitoring temperature-dependent sample properties such as resonant frequency and resistivity. The average electron energy in the 5-mil samples was approximately 2.4 MeV so that E_m, the maximum recoil energy of the tungsten atom, was about 95 eV. For $E_d=47\pm 3$ eV, the displacement threshold energy recently measured for tungsten,[10] the Kinchin and Pease cascade model[11] predicts that some of the primary knock-ons had sufficient recoil energy to produce secondaries, that is, those primaries with $E>2E_d$. For the given E_m and E_d, however, Oen's calculations[12] indicate that the contribution of secondary defect production to the total displacement cross section (between 50 and 70 b) is negligible in comparison to the contribution of primary knock-ons. Thus the effect of the electron irradiation was essentially the production of simple isolated Frenkel pairs with varying separation between the constituents.

III. EXPERIMENTAL RESULTS

A. Internal Friction

The preirradiation internal friction-versus-temperature spectrum for a single crystal with the [100]

[9] P. M. Morse, *Vibration and Sound* (McGraw-Hill Book Co., Inc., New York, 1948), Chap. 4.

[10] C. G. Roberts and P. E. Shearin of the University of North Carolina (private communication).

[11] G. H. Kinchin and R. S. Pease, J. Nucl. Energy 1, 200 (1955).

[12] O. S. Oen, Oak Ridge National Laboratory Report No. ORNL-3813, 1965 (unpublished).

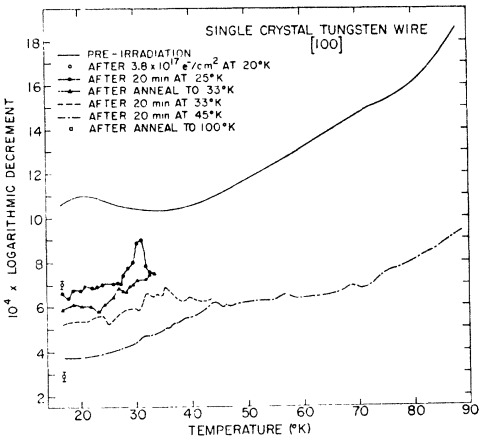

FIG. 3. The δ-versus-T results for the preirradiation and anneal runs on a previously unirradiated [100] single crystal.

direction along its length is shown by the solid curve in Fig. 3. The actual data points taken every 1 to 2 deg were omitted for clarity. The measurements were extended to 90°K in order to cover the temperature range commonly referred to as Stage I in tungsten. The monotonic rise of the decrement with temperature can be attributed to the low-temperature side of the broad dislocation relaxation peak normally found in tungsten[13] and other bcc metals.[14] The effect of electron irradiation on the 17°K mechanical properties of this [100] single crystal is shown in Fig. 4. The decrease of the decrement with flux accompanied by a related resonant-frequency increase can be qualitatively interpreted as irradiation-induced defect pinning of dislocations. The nature of the pinning defects and the difficulty in quantitatively interpreting the flux-dependent results will be considered in the discussion.

After irradiation at 20°K the single-crystal samples were annealed in rapid temperature steps. Since transient effects caused by defect recovery were expected, the fastest warmup rate consistent with data taking was employed. Typically this rate averaged about 1°K per minute between 20 and 45°K. Figure 3 indicates the results of such anneals on a [100] single crystal. For all the internal-friction results the maximum error in the decrement measurements is indicated at the post-irradiation 17°K data point. The significant feature to be observed in Fig. 3 is the relatively large relaxation-type internal-friction maximum at 30°K. This peak had a transient behavior in that after a rapid warmup to 33°K followed by a rapid quench below 20°K, it was essentially unobservable in the next warmup. Also to be noted in Fig. 3 are the small peak structures between 25 and 45°K and the large decreases in the background for anneals above 30°K.

In order to study the 30°K relaxation peak more carefully, all samples were subjected to a high-dose 100°K irradiation before reirradiating them at 20°K. The purpose of this initial irradiation was to pin the dislocations with mobile Stage-I interstitials, thereby suppressing the dislocation contribution to the internal-friction spectrum. Since vacancy motion in tungsten does not occur until above 600°K,[7] this procedure did have the effect of radiation-doping the samples with vacancies. Nonetheless, with a greatly reduced dislocation background it was hoped that the contributions of point defects created in the subsequent 20°K irradiation would be more clearly defined and the source of the 30°K peak identified. For the [100] crystal of Fig. 3, the results of the dislocation pinning, subsequent irradiation, and annealing treatments are shown in Fig. 5. The data only extend from 20 to 50°K because this temperature region appeared to contain the most Stage-I structure (cf. Fig. 3). All curves taken after anneals above 100°K were reproducible on temperature recycling. The significant features to be observed in Fig. 5 are the reappearance of a more prominent 30°K peak, the small rise in background with irradiation, and

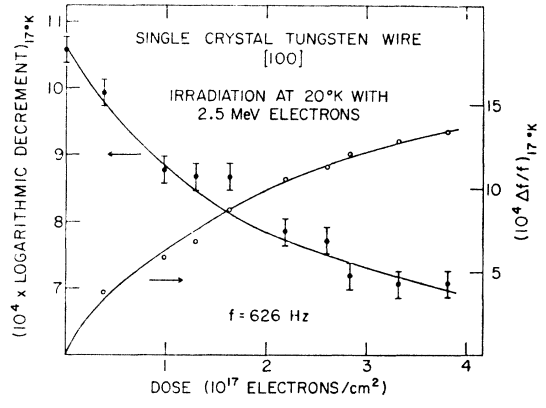

FIG. 4. The effect of electron irradiation at 20°K on the 17°K δ and f of a previously unirradiated [100] single crystal.

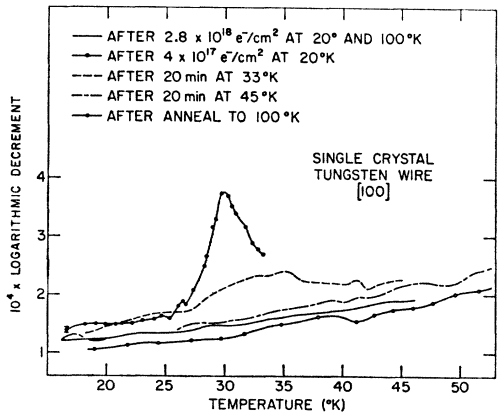

FIG. 5. The δ-versus-T results for the preirradiation and anneal runs on a [100] single crystal which was previously subjected to heavy dislocation-pinning irradiations.

[13] D. R. Muss and J. R. Townsend, J. Appl. Phys. **33**, 1804 (1962).
[14] R. H. Chambers and J. Schultz, Acta Met. **10**, 466 (1962).

the recovery of the irradiation-induced background with annealing. Assuming that a reduced background means pinned dislocations, the reappearance of the 30°K peak implies that it was caused by defects alone. The fact that the supposedly pinned background increased slightly with irradiation and then decreased at higher temperatures suggests that dislocations are not entirely inactive but can interact with newly introduced point defects. It was hoped that clarification of the involved mechanisms would result from a simultaneous study of resistivity and mechanical properties.

B. Simultaneous Measurements

1. Irradiation

For the simultaneous measurements of resistivity, internal friction, and dynamic modulus, two identical polycrystalline samples were mounted side by side as shown in Fig. 1. The initial irradiation for the purpose of dislocation pinning was performed at 30°K. The resistivity was found to increase linearly with electron irradiation up to the final dose level, 2.1×10^{18} electrons/cm^2. Because of experimental difficulties, no systematic anneal runs were performed on either sample. However, the gross resistivity results which were obtained from the initial irradiation and anneal to 300°K are indicated in Run 1 of Table I. This initial treatment not only pinned the dislocations but also radiation-doped the samples, leaving 25% of the irradiation-induced resistivity $\Delta\rho_0$ in the lattice. Presumably this remaining damage consisted of vacancies, trapped interstitials, and possibly interstitial clusters.

During the second irradiation at 20°K, the resistivity again increased linearly with dose but at a higher rate than observed at 30°K. The production rate and final resistivity change are given in Run 2 of Table I. For a tungsten displacement threshold energy of 47±3 eV[10] Oen's cross-section calculations[12] and the 20°K production rate predict that the resistivity per atomic

TABLE I. Resistivity production and recovery.

	Run 1 (30±1°K)	Run 2 (20°K)	Run 1[a] (20°K)
Resistivity due to radiation doping (10^{-8} Ω cm)	0	1.4	0
Production rate [10^{-26} Ω cm/(e^-/cm^2)]	2.74±0.08	3.10±0.02	3.10±0.02
Total irradiation-induced resistivity (10^{-8} Ω cm)	5.66	1.60	6.4
% recovery			
30±1°K	0	13±3	(12±3)[b]
45°K	40	48	47±1
100°K	62	76	66±1
300°K	75		78±1

[a] Theoretical run calculated with a Run-2 production rate and a Run-1 total dose and recovery.
[b] Calculated from difference in the 20 and 30°K production rates.

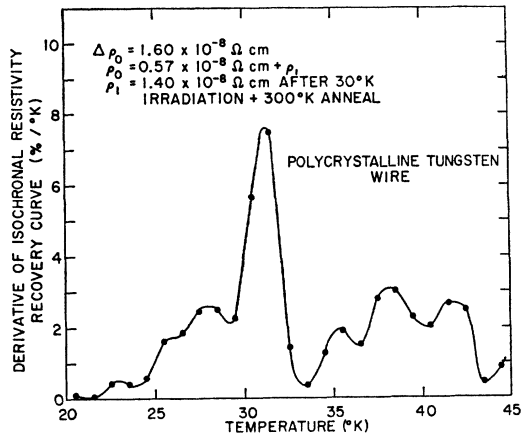

FIG. 6. The derivative of the isochronal resistivity curve for a polycrystalline sample.

percent of tungsten Frenkel pairs lies between 4 and 6 μΩ cm. This result compares well with the value determined by Schultz[7] of 2.5 μΩ cm for 1 at.% of tungsten vacancies.

The 17°K decrement was also observed to increase during the 20°K irradiation, but the increase appeared to be caused by an undetermined combination of dose and time (hours) at temperature. This behavior suggests that near 20°K some irradiation-induced defects were slowly changing their position in the lattice so that their decrement contribution increased but their resistivity contribution remained the same. This δ dependence on dose and time was also observed in the single crystals. Simultaneous frequency measurements showed a frequency decrease Δf proportional to the decrement increase $\Delta\delta$; that is, $(\Delta f/f)/\Delta\delta=-6$.

2. Resistivity Annealing

After the second irradiation, the pair of polycrystalline samples were subjected to an isochronal anneal to 45°K. The anneal was performed in 1°K temperature steps, 20 min at each temperature. The derivative of the isochronal resistivity recovery is shown in Fig. 6. There is a large recovery peak centered at 31°K plus six smaller peaks at 23, 26, 28, 35, 38, and 42°K. The general structure is similar to that observed in the same temperature range by Coltman, Klabunde, and Redman after thermal-neutron irradiation.[15] If the defects contributing to the resistivity annealed with first-order kinetics, then

$$d\rho/dt=\rho K_0\exp[-E_a/kT], \qquad (6)$$

where K_0 and E_a are the rate constant and activation energy for annealing, respectively. Assuming first-order kinetics for the 31°K defects, one can determine their E_a from the peak shape; that is, $E_a=2.4kT_a^2/\Delta T_a$,

[15] R. R. Coltman, C. E. Klabunde, and J. K. Redman, Phys. Rev. 156, 715 (1967).

where ΔT_a is the temperature width of the peak at half-maximum and T_a the temperature at the peak maximum.[16] Knowing E_a, one can also calculate the rate constant K_0 from the relation[17]

$$\ln(K_0 E_a/k\alpha) = E_a/kT_a + 2\ln(E_a/kT_a), \quad (7)$$

where $\alpha = dT/dt$, the equivalent warmup rate for the isochronal run. For the 31°K defects these calculations yielded $E_a = 0.11 \pm 0.01$ ev and $\log K_0 = 14.5 \pm 1.0$. The error due to the shape of the isochronal temperature pulses was found to be negligible. Since $K_0 = A/a$, where A is an appropriate frequency for defect motion ($A \sim 10^{13}$ sec^{-1}) and a the average number of jumps to reach an annihilation center,[18] the 31°K defect required a number of jumps of the order of unity to recover.

After the second irradiation, the gross resistivity recovery as a function of temperature is indicated in Run 2 of Table I. The effect of the radiation doping was determined by assuming that the first irradiation was performed at 20°K with a production rate identical to that observed in the 2nd irradiation. This assumption is justified because both production curves were found to be linear in dose, indicating no dose dependence for the defects which anneal between 20 and 30°K. Recalculation of the recovery percentages that would have been observed for an assumed 20°K first irradiation yields the results in column 3 of Table I. The 30°K value was derived by a comparison of the 30°K and the 20°K production rates. Thus the table indicates that the recovery fractions are essentially the same up to 45°K, but between 45 and 100°K, 10% more recovery occurs after radiation doping. Comparing this result with similar experiments on copper,[19] it appears that long-range interstitial motion does not occur in tungsten until above 45°K.

3. *Mechanical Property Annealing*

Before considering the annealing results on the decrement and frequency of the internal-friction sample, one should discuss the possible effects of irradiation on these properties. Since the only effect of electron irradiation is to introduce simple isolated point defects, any observed changes in decrement and/or modulus (resonant frequency) must be ultimately caused by these defects. Whereas the decrement is only affected by the anelastic behavior of crystal imperfections, the modulus is affected both by anelastic and elastic behavior. Under the category of anelastic behavior fall the mechanisms of stress-induced ordering and defect-dislocation interactions, such as dislocation pinning. Under the category of elastic behavior falls the mechanism of alteration of atomic bonds throughout the lattice by the static presence of point defects. For example, Dienes has predicted that static interstitials and vacancies will increase and decrease the elastic modulus, respectively.[20] Thus an irradiation-induced change in modulus can be composed of two parts, that is, $\Delta M = \Delta M_a + \Delta M_e$, where ΔM_a is the anelastic modulus change and ΔM_e the elastic modulus change. The contribution of the stress-induced ordering of defects to the anelastic modulus change ΔM_{ap} and its associated decrement δ_{ap} are given in Eqs. (2) and (1), respectively. The contribution of point-defect-dislocation interactions to the anelastic modulus ΔM_{ad} and its associated decrement δ_{ad} depends on the theoretical model of the involved mechanism. Without going into detailed models one can generalize by stating that ΔM_{ad} and δ_{ad} have some functional dependence on point-defect concentration and thus are related to each other. Finally the contribution of point defects to the elastic modulus is directly proportional to defect concentration and may be positive or negative depending on the defect type.

In the present experiment, point-defect relaxation effects on the decrement (δ_{ap}) were distinguished from point-defect-dislocation interaction effects (δ_{ad}) by observations of the temperature range over which the effect extended. This is based on the fact that, whereas the stress-induced ordering of point defects gives decrement changes localized in temperature, dislocation related effects are generally much broader and thus appear as extended background changes. For this isochronal anneal of the polycrystalline internal-friction sample, δ was measured during the rapid warmup to the anneal temperature and during the 20 min at temperature. Measurements during warmup detected permanent background changes caused by the recovery of point-defect-dislocation interactions. Measurements at temperature showed time-dependent changes caused both by the recovery of point defects which were subjected to stress-induced ordering, and also by the recovery of point-defect-dislocation interactions.

The recovery of the background decrement (δ_{ad}) as a function of isochronal anneal temperature, shown in Fig. 7, was determined by comparing the data of each consecutive rapid warmup run with the data of the preirradiation warmup run and then plotting the difference at the indicated temperatures. Any observed change was recorded as a change caused by the anneal at the previous isochronal anneal temperature. For clarity the best-fit curves have been employed. The final warmup run after an anneal at 100°K was observed to be essentially identical to the preirradiation run between 20 and 45°K, indicating that in this region complete recovery of the irradiation-induced decrement structure had occurred by 100°K. The significant fea-

[16] R. O. Simmons, J. S. Koehler, and R. W. Balluffi, *Radiation Damage in Solids* (International Atomic Energy Agency, Vienna, 1962), p. 157.

[17] G. J. Dienes and G. H. Vineyard, *Radiation Effects in Solids* (Wiley-Interscience, Inc., New York, 1957), p. 149.

[18] See, for example, G. D. Magnuson, W. Palmer, and J. S. Koehler, Phys. Rev. **109**, 1990 (1958).

[19] J. W. Corbett, R. B. Smith, and R. M. Walker, Phys. Rev. **114**, 1452 (1959); **114**, 1460 (1959).

[20] G. J. Dienes, Phys. Rev. **86**, 228 (1952); **87**, 666 (1952).

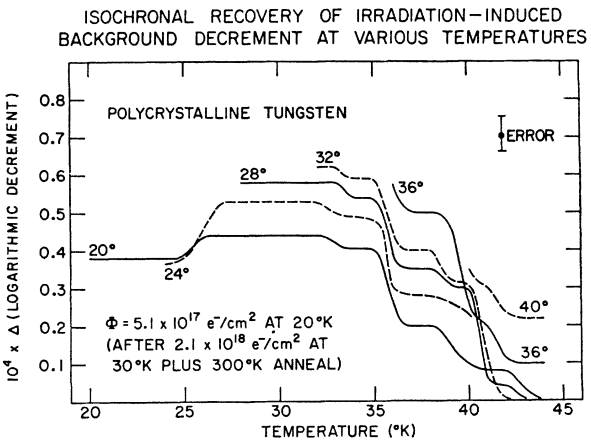

FIG. 7. The isochronal recovery of the irradiation-induced background δ at various temperatures. This polycrystalline sample and the sample of Fig. 6 were subjected to identical irradiation and annealing treatments.

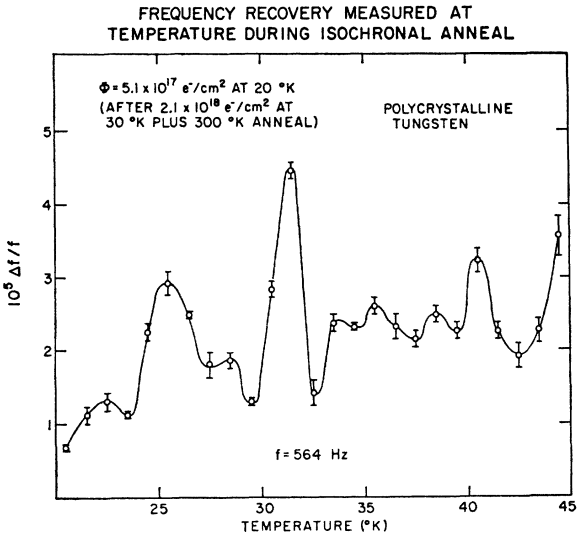

FIG. 9. The isothermal change in f during 20 min at each isochronal anneal temperature for the sample of Fig. 8.

tures to be observed in Fig. 7 are the increase in background at 26°K and the relatively large decreases around 36°K and from 38 to 43°K. It should also be noted that all the changes occurred across a broad temperature range. By comparison with Fig. 6 the background decrement changes of Fig. 7 were found to correspond in temperature to resistivity recovery regions, indicating that the point defects which contribute to a defect-dislocation interaction also contributed to the resistivity. However, the annealing of the 26°K defects increased the background, the annealing of the 28 and 31°K defects produced essentially no change, and the annealing of the 36 to 42°K defects decreased the background. The 36 to 42°K decreases can also be observed in the rapid warmup δ results (cf. Figs. 4 and 5).

The decrement recovery at temperature shown in Fig. 8 was determined as the decrement near $t=0$ less the decrement at $t=20$ min. Thus δ decreased at temperature from 28 to 32°K and 35 to 40°K, and increased slightly near 26°K. Data above 40°K were not taken. The 35 to 40°K and the 26°K changes can be correlated with the background changes (δ_{ad}) observed in Fig. 7. The 28 to 32°K recovery, however, does not show up in the background, indicating that it is localized in temperature and thus not related to dislocations. By comparison with the rapid warmup results, the 28 to 32°K recovery must be produced by the annealing of the defects responsible for the 30°K relaxation peak. The fact that decrement recovery occurred at 28°K implies that the stress-induced ordering of both the 28 and 32°K resistivity defects produced the 30°K internal-friction peak. The disappearence of the localized effects by 33°K again indicates that the defects responsible for the 30°K internal-friction peak annealed out by 33°K.

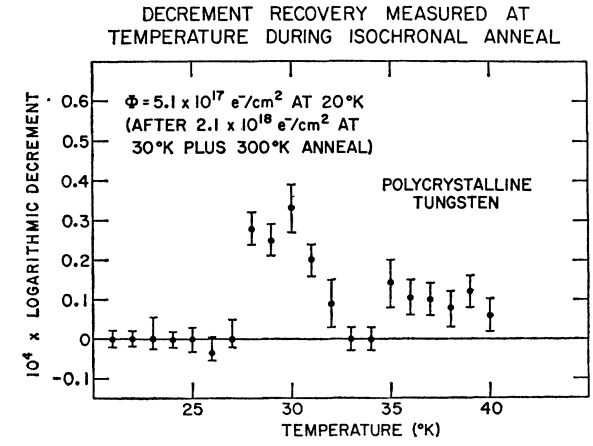

FIG. 8. The isothermal change in δ during 20 min at each isochronal anneal temperature for the sample of Fig. 7.

During the 20-min isochronal anneals, continuous resonant-frequency measurements were also made on the internal-friction polycrystalline sample. The observed frequency increases as a function of temperature as shown in Fig. 9. Comparison with Fig. 6 indicates that a significant similarity exists between the resistivity and frequency annealing, i.e., recovery near 23, 26, 28, 31, and from 33 to 43°K. The 30°K peak was found to have the same half-width for both recoveries. These facts imply that both properties are proportional to defect concentration and therefore to each other. Assuming a direct proportionality to exist, then for the 30°K peak $(\Delta f/f)/\Delta\rho \cong -4\times10^4$ $(\Omega\ \text{cm})^{-1}$, where the minus sign indicates that the frequency increased as the resistivity decreased. This ratio varied between -4×10^4 and -20×10^4 for the other peaks from 20 to 43°K. From a manipulation of Eq. 5,

$$\Delta f/f=\tfrac{1}{2}(\Delta M/M)+\tfrac{1}{2}(\Delta s/s), \qquad (8)$$

where s represents a linear dimension of the sample. Assuming the length change per resistivity change observed in Stage I of copper,[21] $+2\times10^{3}$ $(\Omega\ \mathrm{cm})^{-1}$, applies also to Stage I in tungsten, the maximum $\Delta s/s$ expected for the 30°K resistivity peak in Fig. 6 is -3×10^{-6}. Since this value is of the wrong sign and accounts for only 4% of the $\Delta f/f$ observed at 30°K, it can be concluded that the 30°K peak and in fact all other peaks in the frequency recovery spectrum of Fig. 9 were caused only by changes in the dynamic modulus, i.e., $(\Delta f/f) = (\Delta M/2M)$.

Regarding any correlation between frequency and decrement recovery at temperature, comparison of Figs. 8 and 9 shows that between 20 and 34°K although large changes occur in both properties, these changes do not appear to be related. Since the decrement decreases between 28 and 34°K have been shown to be caused by the recovery of defects subjected to stress-induced ordering, manipulation of Eqs. (1) and (2) predicts a modulus increase of $(\Delta M/M)_{ap}=-\Delta\delta_{ap}/\pi\omega\tau$. Quantitatively the decrement change at 28°K which is below the relaxation peak maximum ($\omega\tau>1$), predicts a frequency recovery of $<5\times10^{-6}$. Since this value is less than the observed value of $\sim2\times10^{-5}$ it would appear that a major portion of the frequency recovery was caused by changes in the elastic modulus ΔM_s. Likewise for the region 20 to 28°K where essentially no point-defect relaxation or background effects were observed (cf. Fig. 8), the frequency recovery is best explained by elastic modulus recovery. Such an interpretation is also supported by the apparent concentration dependence of the recovery structure from 20 to 34°K. However, between 34 and 40°K, the region corresponding to decreases in δ_{ad}, the frequency recovery was probably caused entirely by recovery of ΔM_{ad}. Assuming a linear relation between $\Delta f/f$ and $\Delta\delta$, one finds $(\Delta f/f)/\Delta\delta\approx-3$ which corresponds to $\frac{1}{2}$ of a similar ratio observed during irradiation at 20°K.

C. Dependence on Stress Direction

The transient behavior of the 30°K peak, its localized temperature dependence, and its independence of dislocation background suggest that it was produced by the stress-induced ordering of point defects. Therefore, measurements of the 30°K peak height as a function of external stress direction should determine the orientation configuration of the responsible defects. Since the defects appear to anneal out by 33°K, single crystals were irradiated and annealed in sets of two to insure equal defect concentrations at all times and to prevent discrepancies in anneal times between the samples. The results of such measurements are shown in Figs. 10 and 11.

For set A, consisting of a [100] and a [110] single crystal, the initial heavy irradiation treatments resulted

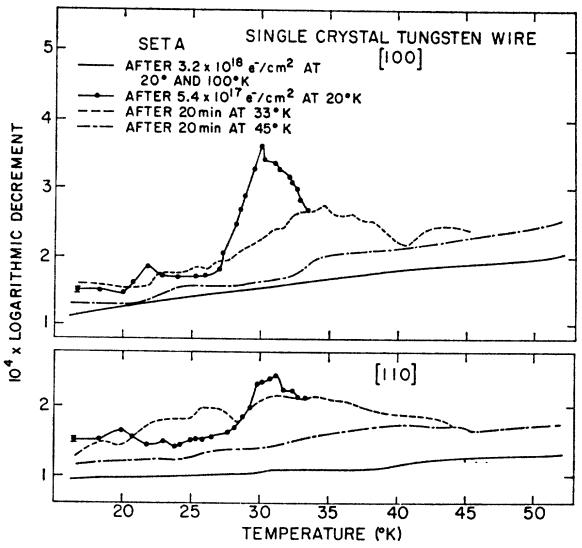

FIG. 10. The δ-versus-T results for the preirradiation and anneal runs on a [100] and a [110] single crystal. Both samples were subjected to identical irradiation and annealing treatments.

in structureless preirradiation backgrounds as indicated by the solid lines of Fig. 10. Irradiation at 20°K, followed by an anneal to 33°K (dotted curve), produced an increase with small structure and revealed the 30°K peak in both crystals, the peak in the [100] sample being the larger. After a 20-min anneal at 33°K, a quench, and a warmup to 45°K, the 30°K peak disappeared from both samples, but the background on the [110] crystal was somewhat higher around 25°K. After a quench from 45°K, the final warmup (dash-dot curve) showed most of the irradiation-induced structure to have essentially disappeared, leaving a background still above the preirradiation value. However, this excess

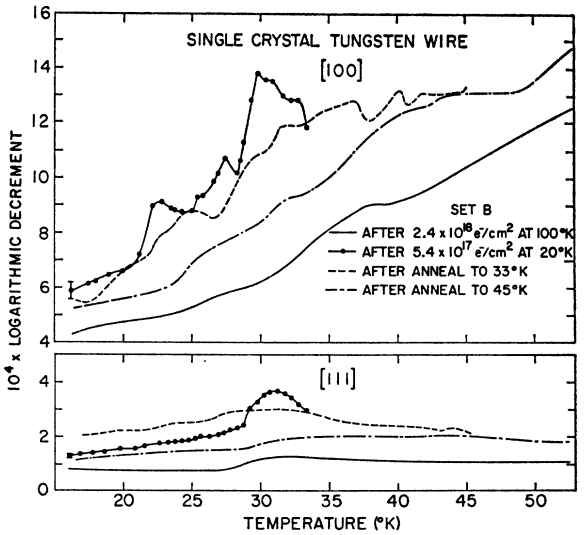

FIG. 11. The δ-versus-T results for the preirradiation and anneal runs on a [100] and a [111] single crystal. Both samples were subjected to identical irradiation and annealing treatments.

[21] R. Hanada and J. W. Kauffman, Appl. Phys. Letters 12, 42 (1968).

decrement eventually annealed out during the warmup to 100°K (cf. Fig. 5).

Set B, consisting of a [100] and a [111] single crystal subjected to essentially the same treatment as set A, yielded the results shown in Fig. 11. The decrement-versus-temperature spectra of this [100] crystal again revealed the 30°K peak plus smaller peaks at 23, 27, 36, and 40°K. Comparison with Fig. 6 indicates correspondence between these small decrement peaks and the resistivity recovery peaks, suggesting that all the resistivity defects can also contribute to the decrement through stress-induced ordering. The fact that these decrement peaks are more evident in this [100] crystal than in the other [100] crystals can be explained by a higher defect concentration as evidenced by the relative heights of the 30°K peak. The decrement spectra of the [111] crystal did not reveal any of the small peaks but did display the 30°K peak about three times smaller than that observed in the [100] crystal. However, during the warmup after the 33°K anneal the [111] background was observed to be higher from 20 to 33°K.

As evident in Figs. 10 and 11 a determination of the 30°K relaxation-strength ratios is difficult because of small peak heights and shifting backgrounds in the [110] and [111] crystals. However, since all four peaks in these figures have essentially the same relative temperature dependence, it can be concluded that they were all caused by the same process. Therefore, since comparison of dotted and dashed curves in the [100] data shows the 30°K peak to begin at 28°K, it follows that the peaks in the [110] and [111] crystals should also begin at 28°K. For this reason Δ_0 ratios were determined by considering the background for the [100] crystals as the decrement observed after the 33°K anneal (dashed curve) and the background for the [110] and [111] crystals as a straight line between the 28 and 33°K data points on the first postirradiation run (dotted curve). This procedure appears to be justified because it yields nearly constant Δ_0 ratio's across the entire peak; that is,

$$\begin{aligned}\Delta_0^{110}/\Delta_0^{100} &\equiv R_{100}^{110} = 0.40 \pm 0.10\,, \\ \Delta_0^{111}/\Delta_0^{100} &\equiv R_{100}^{111} = 0.40 \pm 0.15\,.\end{aligned} \tag{9}$$

IV. DISCUSSION

A. Recovery in Tungsten

Before discussing the mechanical-property results one should attempt to understand the nature and temperature location of the point-defect recovery mechanisms operative in tungsten. Original resistivity recovery measurements on fast-neutron irradiated tungsten by Kinchin and Thompson[22] have shown the existence of three principal low temperature recovery stages: Stage I, 0–100°K; Stage II, 100–600°K; and Stage III, 600–750°K. Thompson[23] suggested that Stage-I annealing should be assigned to interstitials, Stage II to impurity-trapped interstitials, and Stage III to vacancies. Support for interstitial motion below 100°K can be found in the field-ion microscope experiments of Sinha and Müller[24] who observed that irradiation-induced interstitials diffuse out of a tungsten tip between 50 and 90°K. Above 90°K no further interstitial motion was seen. Support for the release of impurity-trapped interstitials between 100 and 300°K can be found in the internal-friction experiments of DiCarlo and Townsend[25] who observed two transient relaxation peaks in deuteron-irradiated tungsten. These peaks existed only in impure samples and were traceable to the stress-induced ordering of interstitial-impurity complexes. Regarding Stage III there is evidence that another form of the interstitial, rather than the vacancy, is the mobile defect. For example, in cold-working experiments Schultz[7] has observed second-order kinetics for Stage III, implying interstitial-vacancy recombination via interstitial motion. Additional support for the Stage-III interstitial motion has been given by Attardo *et al.*[26] who by field-ion microscopy observed interstitial removal during Stage-III recovery of neutron-irradiated tungsten. As for motion of the vacancy itself, Schultz[27] suggests that this process occurs from 600 to 920°C, the temperature range corresponding to recovery Stages IV and V observed after cold working. For the purpose of the present discussion, however, one need only accept the fact that after Stage I in high-purity tungsten, vacancies do not anneal out until above 600°K.

Returning to Stage I, fast-neutron results on tungsten[28] show only broad recovery from 4 to 100°K, presumably attributable to the complicated damage produced by that type of irradiation. Recently, however, from the simple damage produced by thermal neutrons, Coltman *et al.*[15] have found Stage I in tungsten to consist of some ten or more distinguishable substages. In order of decreasing size the five most significant tungsten substages occurred near 16, 62, 11, 31, and 80°K. Whereas the thermal-neutron irradiation revealed four peaks between 20 and 45°K, the finer isochronal temperature steps of the present experiment have revealed at least six in this temperature range. If one assumes that the three point-defect recovery mechanisms generally employed to explain Stage I in copper, that is, close-pair, correlated and uncorrelated recovery,[19] are also operative in other metals regardless of their crystal structure, then each tungsten substage mechanism should be identifiable by its properties.

[22] G. Kinchin and M. W. Thompson, J. Nucl. Energy **6**, 275 (1958).

[23] M. W. Thompson, Phil. Mag. **5**, 278 (1960).

[24] M. K. Sinha and E. W. Müller, J. Appl. Phys. **35**, 1256 (1964).

[25] J. A. DiCarlo and J. R. Townsend, Acta Met. **14**, 1715 (1966).

[26] M. J. Attardo, J. M. Galligan, and J. G. Y. Chow, Phys. Rev. Letters **19**, 73 (1967).

[27] H. Schultz, Mater. Sci. Eng. **3**, 189 (1968/69).

[28] See, for example, A. Granato and K. Lücke, J. Appl. Phys. **27**, 583 (1956).

Turning to the Table-I results, one can observe that radiation doping with vacancies did not enhance recovery until between 45 and 100°K, implying uncorrelated or long-range tungsten interstitial motion occurred somewhere in this temperature range. This conclusion is based on the fact that only the uncorrelated substage in Stage I of copper was observed to be markedly affected by radiation doping. The physical interpretation of this doping effect is that only the uncorrelated interstitials which move long distances are affected appreciably by the excess vacancy concentration introduced by prior irradiation. The assignment of free migration to this temperature range is in agreement with the electron-irradiation results of Neely *et al.*[29] who have observed second-order kinetics during resistivity recovery near 70°K. From the order of the kinetics they conclude that freely migrating interstitials were annihilating with vacancies or being trapped by impurities. Recently Roberts and Shearin[10] have obtained recovery results on electron-irradiated tungsten which indicate a second-order process near 22°K, suggesting long-range interstitial motion in this temperature region. Such an interpretation, however, is inconsistent with the present results which show constant production rates at 20 and 30°K.

If the assumed similarity between tungsten and copper recovery is to hold, the complex recovery below 60°K in tungsten must be assigned to a large variety of close pairs, presumably spread out in temperature (activation energy) due to different initial vacancy-interstitial separations or configurations. The resistivity data of the present experiment do support such an assignment. First, from the results in Table I the recovery between 20 and 45°K was observed to be unaffected by about a fourfold change in $\Delta\rho_0$. This independence of total Frenkel pair concentration is a characteristic of close-pair recovery. Secondly, Table I also indicates that the recovery between 20 and 45°K was not dependent on radiation doping, another indication of close-pair recovery. The physical interpretation for both of these properties is that the mobile close-pair interstitial is only influenced by the strain field of its own vacancy and thus is independent of other damage in the lattice. Thirdly, the width of the 30°K resistivity peak and the assumption of first-order kinetics predicts the number of annealing jumps for the 30°K defects to be of the order of unity, another result consistent wlth close-pair recombination.

In summary, the present resistivity recovery results support the assignment of close-pair recovery in tungsten to the temperature region between 20 and 45°K. The data also bracket uncorrelated recovery between 45 and 100°K. From a comparison with thermal-neutron recovery, the above results would suggest that the peaks below 20°K are also caused by close-pair recovery.

[29] H. H. Neely, D. W. Keefer, and A. Sosin, Phys. Status Solidi 28, 675 (1968).

B. Peak at 30°K

1. Source

The experimental results point to the interstitial members of close-pair Frenkel defects as the source of the 30°K internal-friction peak observed in all samples. First, the peak appears after electron irradiation which has the sole effect of producing simple isolated interstitial-vacancy pairs. Second, for approximately equivalent irradiations and warmup rates, the size of the 30°K peak remains essentially the same although the background changes by an order of magnitude (cf. Figs. 3 and 5). Thus, peak size is independent of dislocation motion, the primary source of the background friction. Finally, simultaneous measurements of decrement and resistivity indicate that the annealing of the 30°K peak proceeded concurrently with resistivity recovery from 28 to 33°K. Since electron irradiation is the production method, any observed resistivity recovery can only be attributed to point-defect annealing. Therefore, since this temperature region can be assigned to close-pair recovery, it follows that this type of defect is necessary for the existence of the 30°K peak.

Regarding the microscopic mechanism that produces the 30°K internal-friction peak, the experimental results indicate that stress-induced ordering of thermally-activated point defects is the most probable process. First, the peak structure is localized in temperature as might be expected for a relaxation peak governed by Eqs. (1) and (3). For example, assuming no defect annealing, the temperature width of a relaxation peak at half-maximum is given by

$$\Delta T_{r0}=2.63kT_m^2/E_r, \tag{10}$$

where T_m is the temperature at the peak maximum. This calculation assumes that only a single relaxation process is active and that $E_r\gg kT_m$. For $T_m\approx 30$°K and E_r between 0.05 and 0.1 eV the theoretical half-width is between 2 and 4°K, a result consistent with the experimental data. Second, the relaxation-strength experiments on the single crystals show a significant orientation dependence for the 30°K peak [cf. Eq. (9)]. Stress-induced ordering theory does predict that certain defect configurations can result in such large orientation effects. However, dislocation motion in certain slip directions and on certain slip planes can also show orientation dependence.[30] For example, for bcc tungsten, assuming a ⟨111⟩ slip direction and either {110} or {112} slip planes, one calculates dislocation relaxation-strength ratios for the single crystals of $\Delta_0^{100}/\Delta_0^{110}=2$ and $\Delta_0^{100}/\Delta_0^{111}=3$. These calculations assume equal dislocation densities on all slip planes. However, a dislocation mechanism can be ruled out not only because equal densities should not be expected in the different crystals but also because the only model for the peak structure

[30] R. R. Coltman *et al.*, Oak Ridge National Laboratory Report No. ORNL-3212, 1961, p. 15 (unpublished).

consistent with other experimental results would involve depinning followed by immediate repinning of dislocations by annealing point defects. Therefore, both the localized temperature effect and the orientation dependence imply that the 30°K peak is due to close-pair relaxation caused by stress-induced ordering. However, since the vacancy by itself has the same symmetry as the lattice and is immobile at these low temperatures, it follows that the close-pair interstitial is the irradiation-induced defect essential to the peak.

It should be pointed out that additional experimental evidence for the existence of a thermally-activated relaxation process would be the observation of the 30°K peak at another frequency. If Eq. (3) is obeyed, the peak structure would then shift in temperature. However, this new frequency would have to be less than 600 Hz so that the shift would be to lower temperatures, and the peak could be observed before the responsible interstitials annealed out. Such experiments were considered and actually attempted, but the problem of microphonic noise pickup at the lower resonant frequencies eliminated the feasibility of employing a flexural mode for the alternating external stress. Although the use of a torsional pendulum was then dictated, the practical difficulties in setting up this apparatus eliminated its use in the present experiment.

2. *Defect Configuration*

Following the discussions of Nowick and co-workers,[4,5] the motion of a point defect in a crystal can result in internal friction only if the symmetry of the local distortions surrounding the defect is lower than that of the crystal. When such an "asymmetric" defect is introduced into a stress-free lattice, it can take one of n positions which although energetically equivalent differ from each other due to the orientation of the strain field of the defect relative to axes fixed in the crystal. The total atomic fraction of these defects can thus be expressed as

$$C=\sum_{p=1}^{n} C_p,$$

where C_p is the fraction in the pth position and $p=1, 2, \cdots, n$. Under zero stress conditions $C_p=C_{p+1}$. A unit concentration of defects in only the pth position or orientation will produce a macroscopic strain in the crystal which can be described by a 3×3 elastic strain tensor $\lambda_{ij}^{(p)}$. This "λ tensor" has components

$$\lambda_{ij}^{(p)}=\partial\epsilon_{ij}/\partial C_p, \tag{11}$$

where

$$\epsilon_{ij}=\sum_{p=1}^{n}\lambda_{ij}^{(p)}C_p$$

are components of the total crystal strain tensor due to defects in all orientations. Since the tensor $\lambda_{ij}^{(p)}$ is a strain tensor, it is symmetric ($\lambda_{ij}^{(p)}=\lambda_{ji}^{(p)}$) and therefore can be diagonalized. In the diagonal form, the diagonal components λ_1, λ_2, and λ_3 are independent of p (i.e., of orientation) and represent the three principle strains of the defect along three mutually perpendicular axes. Thus the asymmetric defect can be specified by the crystallographic directions of its three principle strain axes. For example, the ⟨110⟩ split interstitial has its three principle strains along the ⟨110⟩, ⟨1$\bar{1}$0⟩, and ⟨001⟩ directions.

As a result of its asymmetric strain field a defect can interact with an applied uniaxial stress with an interaction energy which is a function of the defect's orientation. At a temperature high enough to allow defects to change orientation with a relaxation time τ_r [cf. Eq. (3)], the defects will tend to reorient more often into the lowest-energy orientation so that at any instant of time its population will be in excess of the stress-free condition. For an alternating uniaxial stress the energies of the orientations are a function of time so that the excess defect population will tend to reorient toward the orientation with the lowest instantaneous energy. However, because the relaxation time τ_r fixes the rate of defect motion, stress-induced defect reorientation can be out of phase with the applied stress, giving rise to energy losses and internal friction. The magnitude of the friction, expressed by the relaxation strength Δ_0, is proportional to the maximum stress-induced energy difference between orientations and to the anisotropy of the defect's strain field. Expressing this anisotropy in terms of the λ parameters, Nowick and Heller[5] have theoretically derived the Δ_0 values which can be expected from several different types of asymmetric defects in a cubic crystal. The lower symmetry defects which they have considered are of the tetragonal, trigonal, and orthorhombic types. The significant characteristics of these defect types and their calculated relaxation strengths for a [100] and a [111] uniaxial stress are given in Table II. The relaxation strength for a [110] uniaxial stress is not unique but is given by the relation [in terms of the ψ of Eq. (4)],

$$\psi_{\langle uvw\rangle}^{[110]}=\tfrac{1}{4}\psi_{\langle uvw\rangle}^{[100]}+\tfrac{3}{4}\psi_{\langle uvw\rangle}^{[111]}. \tag{12}$$

The six possible theoretical bcc self-interstitial configurations[31] are also listed in Table II according to the properties of their strain fields. From the results of the present experiment which show a 30°K relaxation strength for both a [100] and [111] stress (cf. Fig. 11), it follows from Table II that the 30°K interstitial is probably an orthorhombic defect, producing its maximum distortion in the ⟨110⟩ directions. Thus, the orientation data support a ⟨110⟩ split configuration for the reorienting interstitial at 30°K. However, it would appear that the other close-pair interstitials which also produce peaks in the [100] temperature spectra of Fig. 11 may possess tetragonal symmetry since no corresponding peaks are obvious in the [111] spectra.

[31] R. A. Johnson, Phys. Rev. 134, A1329 (1964).

TABLE II. Asymmetric defects in a cubic lattice.

Defect symmetry	Tetragonal	Trigonal	Orthorhombic
Principal strain directions			
(λ_1)	⟨100⟩	⟨111⟩	⟨110⟩
(λ_2)	⟨010⟩	⟨1$\bar{1}$0⟩[a]	⟨1$\bar{1}$0⟩
(λ_3)	⟨001⟩	⟨11$\bar{2}$⟩[a]	⟨001⟩
Symmetry relations	$\lambda_2=\lambda_3$	$\lambda_2=\lambda_3$	
No. of orientations	3	4	6
Relaxation strength (ψ)[b] versus stress direction [*hkl*]			
[100]	$2(\lambda_1-\lambda_2)^2$	0	$2[\frac{1}{2}(\lambda_1+\lambda_2)-\lambda_3]^2$
[111]	0	$\frac{4}{3}(\lambda_1-\lambda_2)^2$	$(\lambda_1-\lambda_2)^2$
bcc interstitial configurations[c]			
(single atom)	octahedral, tetrahedral	activated crowdion	
(split)	⟨100⟩	⟨111⟩	⟨110⟩

[a] These are not unique directions.
[b] ψ is directly proportional to Δ_0 as shown by Eq. (4) of the text.
[c] See, for example, R. A. Johnson, Phys. Rev. 134A, 1329 (1964).

Although one is tempted to label these interstitials as ⟨100⟩ defects, such a conclusion would be quite tenuous due to the small peak heights and shifting backgrounds. Nevertheless, it can be concluded that the Stage-I interstitials in tungsten do not possess trigonal symmetry; that is, are not in either the ⟨111⟩ split configuration or activated-crowdion configuration.

3. *Defect Properties*

From the directional dependence of the 30°K peak, the relaxation strength ratios R_{100}^{110} and R_{100}^{111} were determined (Eq. 9). The concentration dependence of each Δ_0 in these ratios was eliminated from consideration by subjecting each pair of single crystals to identical irradiation and annealing treatments. The directional dependence of the modulus can also be eliminated because tungsten behaves like an elastically isotropic solid.[32] Therefore the Δ_0 ratios are equivalent to ψ ratios and from Eq. (12) should obey the relation $4R_{100}^{110}-3R_{100}^{111}=1$. This additional condition on the ratios determines their experimental values more precisely; that is, $R_{100}^{110}=0.47\pm0.03$ and $R_{100}^{111}=0.29\pm0.04$. Thus, from Table II,

$$(R_{100}^{111})^{-1}=\frac{(\lambda_1+\lambda_2-2\lambda_3)^2}{2(\lambda_1-\lambda_2)^2}=3.5\pm0.5, \quad (13)$$

which reduces to

$$\frac{\lambda_3-\lambda_1}{\lambda_1-\lambda_2}=+(0.8\pm0.1) \quad \text{or} \quad -(1.8\pm0.1). \quad (14)$$

Since the ⟨110⟩ split interstitial should produce maximum distortion in the ⟨110⟩ directions, that is, $\lambda_1>\lambda_2,\lambda_3$, it follows that the negative solution is the appropriate value.

[32] C. Kittel, *Introduction to Solid State Physics* (John Wiley & Sons, Inc., New York, 1966), 3rd ed., p. 122.

One can obtain further conditions on the λ's by consideration of the dose dependence of the 30°K peak. If δ^{100} is the peak height observed at 30°K in each of the [100] single crystals and if one assumes that δ^{100} is directly proportional to dose, then the experimental results show that

$$d\delta^{100}/d\Phi=(5\pm1)\times10^{-22}/e^-\ \text{cm}^{-2}. \quad (15)$$

Because the defects reorienting at 30°K are also annealing, the observed temperature for the peak maximum (i.e., 30°K) is not the true peak temperature predicted by Eq. (1); that is, $\tau_r(30°)\neq\omega^{-1}$. In other words, the peak maximum is probably an apparent maximum produced by defect recovery, and the true maximum would have occurred at some higher temperature if there were no recovery. Nevertheless, as will be demonstrated shortly, the true maximum probably lies no higher than 34°K. Therefore, from Eq. (1) and a linear extrapolation of the low-temperature side of the peak, $\pi\Delta_0^{100}/2=(1.7\pm0.7)\delta^{100}$ so that from Eq. (4),

$$d\Delta_0^{100}/d\Phi=(v_0M/9kT)\psi_{\langle110\rangle}^{[100]}dC/d\Phi$$
$$=(6\pm3)\times10^{-22}/\text{e}^-\ \text{cm}^{-2}. \quad (16)$$

Since C can be related to the atomic fraction of those close pairs which produce the 31°K resistivity-recovery peak, then for a dose of 10^{17} e$^-$cm^{-2} the polycrystalline results show that between 28 and 33°K, $\Delta C=(1.5\pm0.5)\times10^{-6}$, where the experimental value $\Delta\rho_F/\Delta C=500\pm100\ \mu\Omega$ cm was used for the resistivity per Frenkel pair. Substituting for the other parameters in Eq. (16), one obtains

$$\psi_{\langle110\rangle}^{[100]}=(3\pm2)\times10^{-2}$$
$$=(3.5\pm0.5)\psi_{\langle110\rangle}^{[111]} \quad (17)$$

or combining with Eq. (14)

$$\lambda_1-\lambda_2=0.09\pm0.04,$$
$$\lambda_1-\lambda_3=0.17\pm0.08. \quad (18)$$

Thus it would appear that the 30°K ⟨110⟩ split interstitials are surrounded by nearly isotropic strain fields, and therefore would have been very difficult to detect were it not for the low observation temperature. Finally from the definition of Eq. (11), it follows that

$$\lambda_1+\lambda_2+\lambda_3=\Delta V/v_0\equiv b, \quad (19)$$

where ΔV is the volume expansion produced by each interstitial. If one assumes that the theoretical value for b determined by Johnson[31] for the ⟨110⟩ split interstitial in iron applies also to tungsten, i.e., $b=1.6$, then $\lambda_1\approx0.6$, $\lambda_2\approx0.5$, and $\lambda_3\approx0.4$.

Although the occurrence of recovery probably made it impossible to observe the temperature of the true maximum, T_m, nevertheless one can obtain a good estimate for this temperature from the data and from it infer the energy of reorientation, E_r for the 30°K interstitial. Assuming ΔT_r, the full width at half-

maximum for the 30°K peak, is equal to $\frac{1}{2}$ the estimated full baseline width of the peak, it follows that

$$T_m = \Delta T_r + (27.5 \pm 0.5)°\mathrm{K}. \quad (20)$$

The effect of the asymmetry of a theoretical peak around T_m was omitted because of its negligible contribution to the final result. The start of the 30°K peak, i.e., ($\sim$27.5±0.5°K), was determined by the intersection of the background decrement with a linear extrapolation of the low-temperature side of the peak. It is assumed that in this temperature region appreciable defect recovery had not yet occurred. In general, ΔT_r can be larger than the width expected for a single process, ΔT_{r0}. For example, the authors have found that after electron irradiation $\Delta T_r \approx 1.3 \Delta T_{r0}$ for the tungsten Stage-II peaks which were originally observed by DiCarlo and Townsend[25] and interpreted as peaks produced by interstitial-impurity complexes. Since $\tau_{r0} = 10^{-13}$ to 10^{-15} sec for point-defect reorientation, Eq. (3) predicts $E_r/kT_m = 24 \pm 3$, where the condition at peak maximum, $[\tau_r(T_m)]^{-1} = \omega \approx 3800$ sec^{-1}, was used. Using this last result, Eqs. (10) and (20), and assuming $\Delta T_r = (1.2 \pm 0.2) \Delta T_{r0}$, one obtains $T_m = 31.9 \pm 2.0$°K and $E_r = 0.066 \pm 0.012$ eV. Thus if defect recovery had not occurred, the 30°K peak would have had its maximum somewhere between 30 and 34°K. Also because the 30°K interstitial has a lower reorientation energy than activation energy for recovery ($E_a = 0.11 \pm 0.01$ eV), it can make many reorientation jumps ($\sim 10^7$) for each migration jump. In fact, if this were not the case, internal-friction measurements probably would not have detected this interstitial at all. Finally, the difference between E_r and E_a lends support to the conclusion that the interstitial is in a split configuration. That is, only the split interstitial can make a reorientation jump which is different than its migration jump. The reorientation jump is accomplished by a rotation of the two-atom dumbbell-shaped interstitial around its center of mass; whereas the migration jump is accomplished by a translation of its center of mass. During the rotation and migration the energy barriers E_r and E_a are crossed, respectively.

C. Background Decrement

The decrease in the 17°K background decrement with electron dose for a previously unirradiated sample (cf. Fig. 4) is similar to that observed for copper[33] near 4°K. The interpretation of this effect is clearly the pinning of dislocations by irradiation-induced defects. However, since the pinning is observed at temperatures within and below regions attributed to close-pair recovery, the pinning defects could not have migrated to dislocations but were dynamically deposited there during the irradiation. Leibfried[34] has explained the copper data in terms of focusons, that is, the transport of energy by focusing collisions down rows of close-packed atoms. When the collision sequence is interrupted by a dislocation, the focuson energy is converted into the creation of an interstitial and vacancy which then pin the dislocation. Other mechanisms such as the focused replacement collision[34] and channeling can also be interrupted by dislocations to produce pinning defects. Presumably, all three mechanisms can account in varying degrees for the present first-irradiation tungsten results.

The application of simple dislocation-pinning theory to the low-dose dependence of the decrement and frequency (Fig. 4) is excluded by the results of the second radiation, that is, the anomalous rise in background with dose and time (cf. Fig. 5). Although probably smaller than the effect due purely to pinning, this "rise effect" presumably added its own contribution to the decrement during the first irradiation, producing a total dose dependence unamenable to quantitative analysis. Similar rise effects have been observed in copper by Keefer and Vitt[35] who found the internal friction of an annealed specimen increased both with electron irradiation and subsequent annealing. One might initially attribute the decrement rise to a dislocation depinning process which can occur concurrently with pinning. A simple depinning model would involve the deposition of defects at dislocations which lower the interaction forces between the dislocations and their pinning points. However, since the first irradiation showed a net pinning effect, it follows that during the second irradiation pinning should still be more effective than depinning. Therefore a more tenable interpretation would be that two distinct processes are operative in the dose-dependent results. In the first process, point defects pin dislocations and decrease the friction; while in the second process, defects interact with dislocations in such a manner as to produce a friction rise. The postulation of these processes assumes that because of its broad temperature dependence the background decrement was produced by dislocation motion so that irradiation-induced changes must necessarily evolve from point-defect-dislocation interactions. Whereas both processes make significant contributions in the initial irradiation, only the contribution of the second mechanism should be evident in the irradiations performed after minimum backgrounds were attained. The general annealing characteristics of the second process can be found in Figs. 5, 7, 8, 10, and 11 which all indicate major recovery at 36°K and from 38 to 43°K. Similar recovery was also found after the first irradiation for the [100] crystal of Fig. 3, supporting the existence of the rise effect during the low-dose region. In fact, without the subsequent data these first irradiation spectra could have been interpreted as evidence of dislocation pinning from 35 to

[33] See, for instance, D. O. Thompson, T. H. Blewitt, and D. K. Holmes, J. Appl. Phys. **28**, 742 (1957); A. Sosin, *ibid.* 33, 3373 (1962).

[34] G. Leibfried, J. Appl. Phys. **31**, 117 (1960); **30**, 1388 (1959).

[35] D. Keefer and R. Vitt, Acta Met. **15**, 1501 (1967).

45°K.[36] However, this interpretation now appears to be invalid not only because of the existence of the rise effect, but also because long-range interstitial motion in tungsten does not seem to occur until about 45°K. Finally, although the exact nature of the rise-effect mechanism is not clear, comparison of Figs. 6 and 8 indicates that the irradiation-induced background decrement anneals during close-pair recovery substages, suggesting that close-pair configurations are essential to the mechanism. The background reductions between 35 and 45°K might then be interpreted as the disappearance of defect-dislocation interactions through mutual annihilation of the close-pair constituents. On the other hand, the decrement increases near 26°K might suggest the conversion of one close-pair configuration into another more stable configuration which in its interaction with dislocations produces a larger decrement.

V. CONCLUSIONS

For an applied stress frequency of about 600 Hz, the results of the present research on Stage I in tungsten have revealed the existence of a prominent irradiation-induced internal-friction peak near 30°K. Peak properties such as its temperature half-width, dependence on stress direction, apparent independence of dislocation background, and radiation doping, and disappearance during close-pair resistivity recovery imply that it was produced by the stress-induced ordering of close-pair interstitials. Directional-dependence results suggest that the 30°K interstitials are not trigonal defects, that is, crowdions, but probably are orthorhombic defects in general and ⟨110⟩ split interstitials in particular. The split configuration for this interstitial is also supported by activation energy determinations which show its reorientation energy to be lower than its migration energy. In fact, were it not for a combination of this latter result and the low-observation temperature, internal-friction measurements in the employed frequency range would probably not have detected the interstitial at all. This conclusion is especially true in the case of electron irradiation since at these low irradiation temperatures it becomes impractical to use electrons to produce total defect concentrations greater than those attained here ($\sim 10^{-4}$). Nevertheless, the present results do suggest that, given a high enough defect concentration and a low enough stress frequency, self-interstitials in the bcc metals, like impurity interstitials, can be detected and studied by internal-friction techniques.

[36] J. A. DiCarlo, C. L. Snead, Jr., and A. N. Goland, Bull. Am. Phys. Soc. 13, 381 (1968).

ACKNOWLEDGMENTS

The authors wish to acknowledge the experimental assistance of the Dynamitron technicians and J. Palmer of the Instrumentation Department. One of the authors (J.A.D.) would like to express his thanks to the National Aeronautics and Space Administration for its financial support during the latter stages of this work.

PHYSICAL REVIEW VOLUME 178, NUMBER 3 15 FEBRUARY 1969

Singularities in the X-Ray Absorption and Emission of Metals. I. First-Order Parquet Calculation

B. ROULET, J. GAVORET, AND P. NOZIÈRES
Groupe de Physique des Solides E.N.S., Faculté des Sciences de Paris, 9, Quai Saint Bernard, Paris (5è), France*
(Received 22 August 1968)

X-ray emission and absorption spectra in metals may display singularities near the Fermi-level threshold. These singularities, predicted by Mahan, are due to final-state interactions between conduction electrons and the localized disturbance created by the x ray. The effect is treated within a simple model by the methods of perturbation theory. It is shown that even to lowest order one must sum the so-called parquet diagrams, in close analogy with the Abrikosov theory of the Kondo effect. Mahan's prediction is confirmed, and its validity discussed. Various secondary effects which could blur the singularity are analyzed.

I. INTRODUCTION

THE problem of x-ray absorption or emission in solids has been widely studied in the past thirty years. It has been recognized at an early stage that the electron interaction played an important role. For instance, in the ordinary Auger effect, the x-ray transition is accompanied by the excitation of one extra electron (giving rise to satellite lines and to spectral broadening). Sometimes the Auger effect may display a *collective resonance*, the excited electron being replaced by a plasmon.[1] A detailed review of these various phenomena has been given by Parratt.[2]

In metals, the emission and absorption spectra dis-

* Laboratoire Associé au Centre National de la Recherche Scientifique.

[1] P. Longe and A. J. Glick (to be published).

[2] L. G. Parratt, Rev. Mod. Phys. 31, 616 (1959).